molecular pharmaceutics

Article

pubs.acs.org/molecularpharmaceutics

Advanced Cardiovascular Stent Coated with Nanofiber

Byeongtaek Oh and Chi H. Lee*

Division of Pharmaceutical Sciences, School of Pharmacy, University of Missouri—Kansas City, Kansas City, Missouri 64108, United States

ABSTRACT: Nanofiber was explored as a stent surface coating substance for the treatment of coronary artery diseases (CAD). Nanofibers loaded with nanoparticles containing β-estradiol were developed and exploited to prevent stent-induced restenosis through regulation of the reactive oxygen species (ROS). Eudragit S-100 (ES), a versatile polymer, was used as a nanoparticle (NP) base, and the mixtures of hexafluoro-2-propanol (HFIP), PLGA and PLA at varying ratios were used as a nanofiber base. β-Estradiol was used as a primary compound to alleviate the ROS activity at the subcellular level. Nile-Red was used as a visual marker. Stent was coated with nanofibers produced by electrospinning technique comprising the two-step process. Eudragit nanoparticles (ES-NP) as well as 4 modified types of NP-W (ES-NP were dispersed in H_2O, which was mixed with HFIP (1:1 (v/v) and then subsequently added with 15% PLGA), NP-HW (ES-NP were dispersed in H_2O, which was mixed with HFIP (1:1 (v/v)) already containing 15% PLGA), NP-CHA (ES-NP with a chitosan layer were added in H_2O, which was mixed with HFIP (1:1 (v/v)) containing 15% PLGA), and NP-CHB (ES-NP with a chitosan layer were added in H_2O, which was mixed with HFIP (1:1 (v/v)) containing the mixture of PLGA and PLA at a ratio of 4:1) were developed, and their properties, such as the loading capacity of β-estradiol, the release profiles of β-estradiol, cell cytotoxicity and antioxidant responses to ROS, were characterized and compared. Among composite nanofibers loaded with nanoparticles, NP-CHB had the maximal yield and drug-loading amount of 66.5 ± 3.7% and 147.9 ± 10.1 μg, respectively. The nanofibers of NP-CHB coated on metallic mandrel offered the most sustained release profile of β-estradiol. In the confocal microscopy study, NP-W exhibited a low fluorescent intensity of Nile-Red as compared with NP-HW, indicating that the stability of nanoparticles decreased, as the percentage volume of the organic solvent increased. Nanofibers incorporated with β-estradiol yielded a high endothelial proliferation rate, which was about 3-fold greater than the control (without β-estradiol). The cells treated with the enhanced level of H_2O_2 (>1 mM: as ROS source) were mostly nonviable (81.1 ± 12.4%, $p < 0.01$), indicating that ROS induce cell apoptosis and trigger the rupture of atheroma thin layer in a concentration dependent manner. Nanofibers containing β-estradiol (0.5 mM) lowered cellular cytotoxicity from 25.2 ± 4.9% to 8.1 ± 1.4% in the presence of 600 μM H_2O_2, and from 86.8 ± 8.4% to 59.4 ± 8.7% in the presence of 1.0 mM H_2O_2, suggesting that β-estradiol efficiently protected hPCECs from ROS induced cytotoxicity. The level of NO production in hPCECs in the presence of β-estradiol after 6 days of incubation was much greater than that of the control without β-estradiol. In summary, nanofibers loaded with nanoparticles containing β-estradiol could be used as a suitable platform for the surface coating of a cardiovascular stent, achieving enhanced endothelialization at the implanted sites of blood vessels.

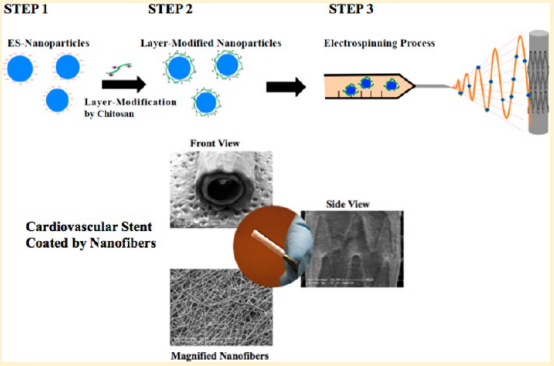

KEYWORDS: *nanofibers, stent coating, β-estradiol, ROS induced cytotoxicity*

1. INTRODUCTION

Coronary artery diseases (CAD) induced by generic factors and dietary habits remain a disease with a serious and potential fatal rate.[1,2] Among CAD, atherosclerosis is the primary source of heart diseases, causing serious pathological symptoms, such as myocardial infarction and angina.[3] Atherosclerosis could be gradually accelerated when cholesterol in the bloodstream is accumulated onto the endothelial surface of coronary artery, narrowing the diameter of blood vessel and building a high pressure.[4] Atheroma composed of deposited cholesterol on the endothelial surface could be ruptured, as the accumulation of cholesterol increases.[5] Eventually, coronary artery will be blocked by platelet adhesion due to the collapse of atheroma mediated through anti-inflammatory response.

To date, angioplasty has been widely used for the treatment of atherosclerosis. The implantation of a stent coated with antithrombogenic agents into the infected lesion has been explored to regulate platelet aggregation.[6] However, stent implantation in the long run stimulates smooth muscle cell migration and the rupture of the atheroma thin layer, causing thrombosis and restenosis (i.e., renarrowing of blood vessels).[7,8] Even though numerous advanced strategies, such as antithrombogenic agents or immunosuppressive drugs including sirolimus onto the surface of the stent via the spray-drying method and electrophoretic deposition (EPD) techniques, have been attempted for drug-eluting stent (DES) and some of them are effective, there still remains an inherent need for advanced means against in-stent restenosis and thrombosis.[8−12]

Received: April 18, 2013
Revised: August 12, 2013
Accepted: September 19, 2013
Published: September 19, 2013

Recently, hormone replacement therapy has been considered as a viable strategy for the treatment of cardiovascular diseases.[13] The general area of our interest lies on the mechanisms behind stimulus-triggering effects of hormonal agents, whose functional properties include the regulation of reactive oxygen species (ROS).[14−16] Since ROS could induce the procoagulant process and the apoptosis of endothelial cells (ECs), an increase of the ROS level would have negative effects on ECs and smooth muscle cells (SMCs).[17,18] Although the Women's Health Initiative (WHI) reported no cardiovascular benefit from hormone replacement therapy (HRT) from the observational studies in 2002, it was recently announced that females treated by HRT early after menopause using β-estradiol had significantly alleviated the risk of heart failure, mortality, and/or myocardial infarction. In addition, the result confirmed that there are no obvious side effects, such as cancer, venous thromboembolism, or stroke.[19]

As matrix metalloproteinases-2 and -9 (MMP-2 and -9) are able to destroy the atheroma thin layer, the enhanced expression of MMP-2 and -9 triggered by ROS caused the rupture of the atheroma formation. It was reported that β-estradiol greatly influences ROS activities, leading to the downregulation of MMP-2 and -9 expression triggered by ROS.[20] The suppressive activity of ROS by β-estradiol has been observed from various cell lines including mesenchymal stem cells, adipose tissue-derived stem cells, cardiomyocyte and bovine aortic endothelial cells.[21−24]

The first human trial with an estrogen-eluting stent displayed a lower rate of restenosis and revascularization.[25] However, two clinical trials with randomized trials showed that β-estradiol did not exert enough activity to overcome restenosis and pro-inflammatory responses, resulting in no difference in therapeutic outcomes from the control.[14,26] The low effectiveness of estrogen eluting stent against restenosis and proinflammatory responses in previous trials was attributed to the following: (1) the biological effect of β-estradiol was vanished through the coating process, and (2) the loaded dose of β-estradiol was too low to be effective. Hence, the novel strategies for hormone replacement therapy should be able to deliver the sufficient dose of β-estradiol without losing its efficacy for a longer period of time.[27]

Stent surface coating of both the inside and the outside of metallic surface has received a little attention from the biomedical field working on coronary artery angioplasty. Nanofiber has emerged as a novel carrier for tissue regeneration. As compared with traditional approaches, such as bare-metal stent (BMS) and drug-eluting stent (DES), nanofiber has various advantages: (1) it can provide a greater surface area, since a whole surface area can be covered by nanofiber, and (2) as turbulent blood flow can intervene with laminar flow, stents coated with nanofiber will provide steady and smooth flow through alleviating restenosis and plaque progression, and remain the cornerstone in interventional cardiology.[28]

In this study, nanofiber was explored as a stent surface coating substrate for the treatment of coronary artery diseases (CAD). Nanofibers loaded with nanoparticles containing β-estradiol have been developed to regulate the ROS activity at the subcellular level and prevent stent-induced restenosis. The layer modification via dual-nano coating technique has been considered as an efficient strategy to protect the nanoparticles from being degraded and triggering initial burst release by strong organic solvent or acidic environment.[29] One of the versatile polymers is chitosan, which showed positive charge under acidic environment, not only enhancing the stability of nanoparticles in organic solvent but also achieving sustained drug release profiles from them. Eudragit S-100 (ES), a versatile ionizable polymer, was used as a nanoparticle (NP) base due to its unique dissolution behavior under varying pH environment.[30] ES-NP were sparsely dissolved in acidic solution and, thus, stable under the acidic condition in which the layer modification with chitosan occurred, whereas they are well dissoluble (whose rate can be properly controllable and sustainable) in neutral pH of blood. The mixtures of hexafluoro-2-propanol (HFIP), PLGA and PLA at varying ratios were used as a nanofiber base.[31−33] Nile-Red was used as a visual marker. The stent was coated with nanofibers produced by the electrospinning technique comprising a two-step process.

2. METHODS

2.1. Materials. Eudragit S-100 was purchased from Rohm (Germany). Poly(DL-lactic acid) (PLA) was purchased from Polyscience. Nile-Red, gelatin type B (from bovine skin), Pluronic F-127, 1,1,1,3,3,3-hexafluoro-2-propanol (HFIP), dimethyl sulfoxide (DMSO), β-estradiol (E2), sulfanilamide and *N*-(1-naphthyl)ethylenediamine dihydrochloride were purchased from Sigma-Aldrich (St. Louis, MO). Poly(DL-lactic-*co*-glycolic acid) (50:50) (PLGA) was purchased from Lakeshore Biomaterials (Birmingham, AL).

Human primary coronary artery endothelial cells (hPCECs) (PCS-100-200), vascular cell basal medium (PCS-100-030) and endothelial growth kit BBE (PCS-100-040) were purchased from ATCC. All other reagents and solvents were of analytical grade.

2.2. Stent Coated with Nanoparticle-Loaded Nanofiber. *2.2.1. Preparation of Nanoparticles.* The modified quasi-emulsion solvent diffusion technique was used for preparation of Eudragit nanoparticles (ES-NP).[30] Briefly, 2.5% (w/v) Eudragit S-100 (ES) and 0.5% (w/v) β-estradiol (E2) were dissolved into 150 μL of methanol. The water phase solution was prepared by dissolving 0.5% (w/v) Pluronic F-127 and 0.15% (w/v) gelatin (type B) into 350 μL of DI water (pH = 3.0), to which 1 mL of HCl was additionally added. The oil phase solution was added into the water phase solution in a dropwise manner. The mixture was kept at room temperature for 24 h with continuous magnetic stirring to evaporate residual organic solvent. The solution containing ES-NP was centrifuged twice at 14,000 rpm for 30 min. The supernatant solution was removed, and the remnant was resuspended in distilled water (500 μL). Nanoparticle suspension was freeze-dried for 24 h and stored until further usage.

Eudragit nanoparticles (ES-NP) as well as 4 modified types of nanofiber solutions (NP-W, NP-HW, NP-CHA, NP-CHB) were prepared. For NP-W, ES-NP were dispersed in DI water (500 μL), which was mixed with HFIP (1:1 (v/v)) and then subsequently added with 15% PLGA, and for NP-HW, ES-NP were dispersed in DI water (500 μL), which was mixed with HFIP (1:1 (v/v)) already containing 15% PLGA, with the final volume of 1 mL.

For NP-CHA and NP-CHB, freeze-dried ES-NP were dispersed in 0.1 M sodium acetate buffer solution (SA buffer; pH = 4.0, 100 μL) and then blended with chitosan solution (0.5% (w/v)). The residual chitosan was removed via ultracentrifugation, and the pellets were redispersed in DI water (500 μL). The HFIP solutions (500 μL) containing a mixture of PLGA and PLA at varying ratios were prepared as described in Table 1A. NP-CHA (ES-NP with a chitosan layer were added in H_2O, which was mixed with HFIP (1:1 (v/v)) containing 15% PLGA) and NP-CHB (ES-NP with a chitosan layer were added in H_2O, which was added with HFIP (1:1 (v/v)) containing the mixture

dx.doi.org/10.1021/mp400231p | *Mol. Pharmaceutics* 2013, 10, 4432−4442

Table 1. Characterization of Nanofibers (A) and Nanoparticles (B)[a]

(A) Nanofibers

	ratio (15% (w/v))						
	PLGA	P(D,L)LA	stability of ES-NP in HFIP (%)	amount of drug in ES-NP(μg)	recovery yield (%)	loaded drug per stent (μg)	diameter distribution (nm)
bare NF[b]	1	0	–	–	49.8 ± 1.2	74.6 ± 18.5	322.5 ± 91.5
NP-W[c]	1	0	32.6 ± 2.0	252.2 ± 15.7	–	–	–
NP-HW[d]	1	0	87.4 ± 4.1	672.25 ± 31.4	51.2 ± 2.8	132.9 ± 3.1	529.7 ± 242.2
NP-CHA[e]	1	0	94.9 ± 2	719.95 ± 18.1	54.7 ± 4.6	127.3 ± 18.4	249.3 ± 123.9
NP-CHB[f]	4	1	96.4 ± 2.4	733.27 ± 1.52	66.5 ± 3.7	147.9 ± 10.1	–

(B) Nanoparticles

	av size (d, nm)	PDI	count rate (kcps)	yield (%)	zeta potential (mV)	entrapment efficiency (%)	loaded drug (μg)
ES-NP	376.4 ± 23.7	0.32 ± 0.04	189.4 ± 0.8	69.6 ± 2.1	−12.9 ± 1.2	73.6 ± 1.4	781.9 ± 39.4
ES-NP with chitosan	541.5 ± 82.3	0.29 ± 0.01	275.9 ± 4.4	–	+18.1 ± 0.8	–	–

[a]"–" indicates that no data were available. Data are shown with mean ± SD (n = 3). [b]For nanofiber without nanoparticles (bare-NF which is assigned as "BNF"), β-estradiol (1% (w/v)) was directly dissolved into the mixture solution (1 mL) of HFIP and PLGA (15% (w/v)). [c]ES-NP were dispersed in H_2O, which was mixed with HFIP (1:1 (v/v)). The mixture was subsequently added with 15% PLGA. [d]ES-NP dispersed in 500 μL of H_2O was added in 500 μL of HFIP already containing 15% (w/v) of PLGA. [e]Chitosan layered ES-NP were dispersed in 500 μL of H_2O, and then added in 500 μL of HFIP already containing 15% (w/v) of PLGA. [f]Chitosan layered ES-NP were dispersed in 500 μL of H_2O, and then added in 500 μL of HFIP already containing 12% (w/v) of PLGA and 3% (w/v) of PLA (4:1).

of PLGA and P(D,L)LA at a ratio of 4:1) were prepared, and their properties, such as the loading capacity of β-estradiol, the release profile of β-estradiol, cell cytotoxicity and antioxidant responses to ROS, were characterized.

2.2.2. Degradation Profiles of Nanoparticles. To investigate the stability of nanoparticles in the organic solvent, the degradation profiles of nanoparticles in the organic solvent mixture were examined through the ultracentrifuge technique performed at 14,000 rpm. The supernatant was diluted with the methanol solution at a ratio of 1:100. Then, it was spectrophotometrically analyzed using UV–vis at 270 nm. The drug concentration in supernatant was used for the assessment of stability of nanoparticles in the organic solvent.

For graphical assessment of morphology and drug distribution, nanoparticles were loaded with Nile-Red, whose lipophilic properties are similar to those of β-estradiol. The intensity of Nile-Red was examined by fluorescent microscopy (Leica DMI 3000B) (Ex and Em are 485 nm and 525 nm, respectively) and Nikon TE-2000U scanning fluorescence confocal microscope (Nikon Inc., Melville, NY).

2.2.3. Electrospinning Technique for Stent Surface Coating. As previously described, four types of ES-NP solutions (i.e., NP-W, NP-HW, NP-CHA, NP-CHB) were prepared for the nanofiber electrospinning solutions. The electrospinning process for stent coating could be divided into two steps.[34] Frist, nanofiber by electrospinning was deposited onto a metallic wire mandrel (16 gauge width and 8 cm length), which was covered by nylon yarn. The total volume of 500 μL was electrospun under the specified processing conditions including potential difference (of voltage) (i.e., 10 kV derived from the difference between positive (+15 kV) and negative (−5 kV) supplied from a Gamma voltage supplier (Ormond Beach, FL)), flow rate (0.6 mL/h) and distance (10 cm) between syringe tip and collector and rotating speed (1800 rpm), as shown in Figure 1. After half of the total volume was consumed to fabricate inner-side meshes, the mandrel was kept at room temperature for an hour.

In the second step, the stent was carefully inserted into the center of the mandrel. The remaining solution was electrospun under the same conditions as the aforementioned parameters. The formulation deposited onto the mandrel was transferred to the vacuum drying container and kept for 7 days to evaporate the residual solvent in the formulation. After 7 days, the nylon yarn was carefully removed to produce a small but sufficient space through which the coated stent is smoothly detached from the mandrel.

For nanofiber without nanoparticles (bare NF, which is assigned as "BNF"), β-estradiol (1% (w/v)) was directly dissolved into the mixture solution (1 mL) of HFIP and PLGA (15% (w/v)). The rest of the procedures are the same as those for nanofiber containing nanoparticles. All samples were prepared in triplicate.

2.3. Characterization of Physicochemical Properties of Nanoparticles and Nanofibers. The physicochemical properties of nanoparticles were characterized using the methods previously used in our laboratory.[30,32] The entrapment efficiency and drug loading capacity of nanoparticles were spectrophotometrically analyzed at a wavelength of 270 nm using Spetronic 20D (ThermoScientific, Waltham, MA).

The recovery yield of varying formulations (i.e., bare NF, NP-W, NP-HW, NP-CHA and NP-CHB) from the electrospinning solution was determined and compared for their electrospinnability. After nanofibers were accumulated on the mandrel, the assembled nanofibers were weighed and the weight was used as W_o, whereas the initial amount of PLGA applied to the electrospinning solution was used as W_s in the equations.

The weight loss of nanofibers immersed in PBS was assessed to investigate the degradation rate of those formulations for specific time intervals. Before being immersed in PBS, the initial weight of nanofiber-coated stents were measured and used as the initial weight of stent coated by nanofibers (W_i). After specific time intervals, the stents were taken out and transferred to the vacuum-drying chamber for a week to fully remove the residual moisture, and then the weight of the stent was remeasured, which was utilized as a dried weight of stent after hydrolysis (W_d). The recovery yields and weight loss were calculated using the following equations.

$$\text{recovery yields (\%)} = [(W_s - W_o)/W_i] \times 100$$

where W_s is the initial weight of applied polymers and W_o is the weight of accumulated nanofiber meshes on the mandrel with residual solvent evaporated, and

$$\text{weight loss (\%)} = [(W_i - W_d)/W_d] \times 100$$

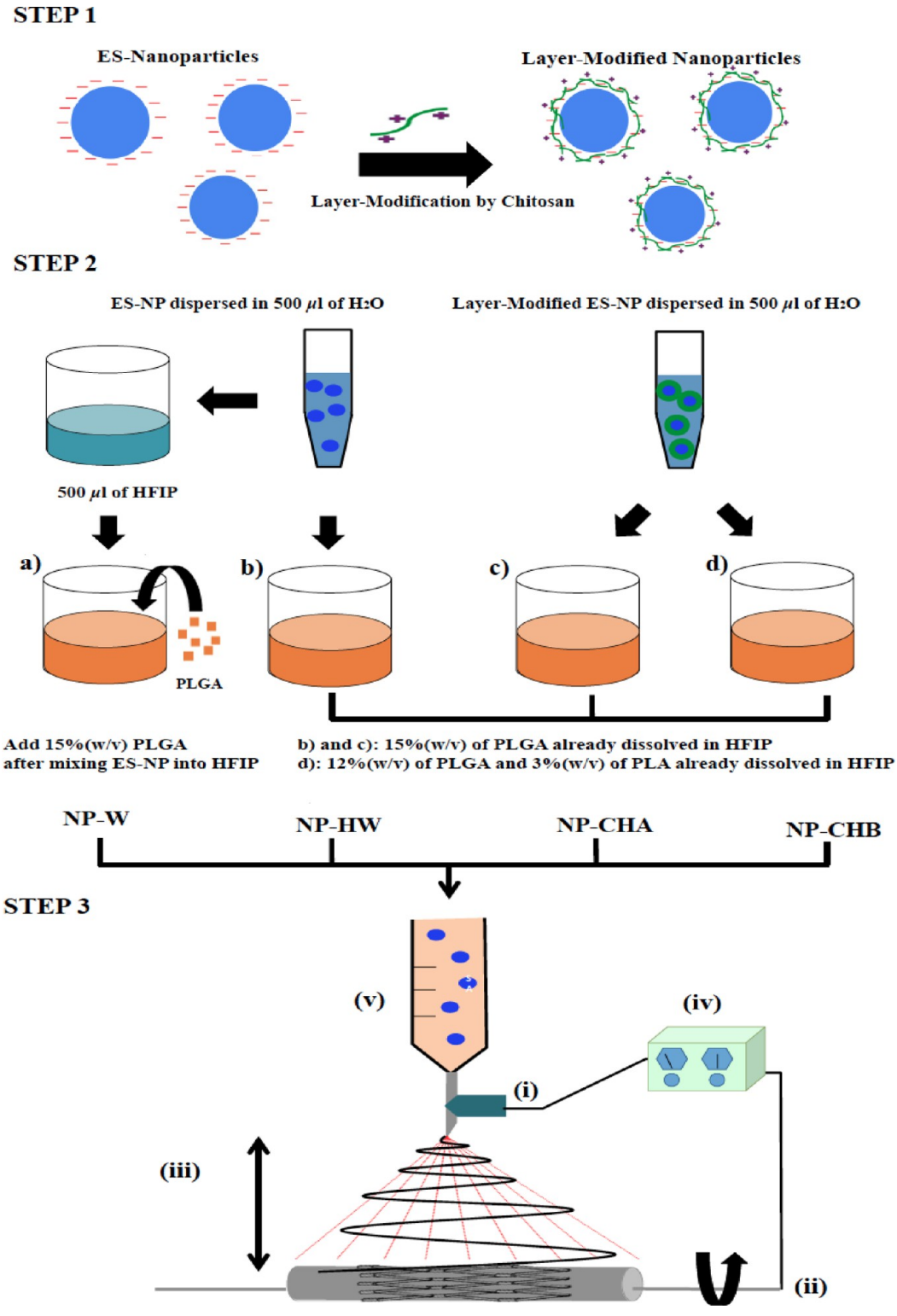

Figure 1. Schematic representation of the stent coating strategy. (Step 1) Preparation of ES nanoparticles and layer-modified ES nanoparticles. (Step 2) Preparation of solutions for electrospinning. (Step 3) Cardiovascular stent coating strategy through electrospinning: (i) flow rate; (ii) rotating speed; (iii) distance between syringe tip and collector; (iv) voltage gradient; (v) total volume of solution.

where W_i is the initial weight of stent coated by nanofibers and W_d is the weight of stent coated by nanofibers with fully residual moisture dried.

The size, distribution and zeta-potential of nanoparticles were examined using dynamic light scattering (DLS) (Zetasizer Nano ZS, Malvern Instruments Ltd., Worcestershire, U.K.), whereas morphological properties were analyzed using scanning electron microscopy (ESEM, XL 30, Hillsboro, OR) and transmission electron microscopy (TEM, JEOL 1200-EX II equipped with goniometric specimen stage).

2.4. Mechanical Characteristics of Varying Nanofiber Types. The mechanical properties of four types of nanofibers

dx.doi.org/10.1021/mp400231p | *Mol. Pharmaceutics* 2013, 10, 4432−4442

made of varying NP solutions (i.e., NP-W, NP-HW, NP-CHA, NP-CHB) were examined using the SSTM-5000 mechanical property analyzer (United Calibration Corporation, CA) with a 150 lb load cell. The samples were tightly fixed to the grip of the analyzer using cyanoacrylate adhesive (Zapit, Dental Ventures of America, Corona, CA). The stress−strain of the samples was measured at a testing rate of 0.5 mm/min at room temperature.[35]

2.5. In Vitro Drug Release Study. Drug release profiles (n = 3) were monitored under pseudophysiological conditions immersed in PBS (pH = 7.4) at 37 °C (onto continuous rotating plate at 120 rpm). Stents coated with nanofibers were immersed into eppendorf tubes (1 mL) containing 1 mL of phosphate buffer solution (pH = 7.4) at 37 °C with continuous shaking at 120 rpm. A fixed volume of the release medium was withdrawn and replenished with the same volume of the fresh PBS solution. All samples were prepared in triplicate and analyzed using UV−vis.

2.6. In Vitro Cellular Response. *2.6.1. Preparation of Cell Lines.* To prepare the cell culture medium, the basal medium was properly mixed with endothelial cell growth kit-VEGF. Briefly, supplement growth kit containing bovine brain extract (BBE) (0.2%), rhEGF (5 ng/mL), L-glutamine (10 mM), heparin sulfate (0.75 unit/mL), hydrocortisone hemisuccinate (1 μg/mL), fetal bovine serum (2%) and ascorbic acid (50 μg/mL) was thawed in the water bath at 37 °C. The medium was gently mixed with growth supplements and kept in the refrigerator at 4 °C. hPCECs were cultured under the standard cell culture conditions (5% CO2 and humidified air at 37 °C).

2.6.2. Evaluation of the Cellular Responses to Nanofiber-Coated Formulations. To assess the cellular responses to nanofibers as well as nanofiber-coated stent, appropriate nanofiber meshes were prepared on the circular glass coverslips. Based on the outcomes of the drug release study, nanofibers from NP-CHB, which showed the maximal yield rate and drug loading capacity, were selected for continuous cellular evaluation studies. Nanofibers were collected onto the circular type of cover glasses (5 mm in diameter) (Thomas Scientific, NJ). After the residual solvent was completely evaporated, the glasses were embedded into 96 wells. To prevent the nanofibers from being floated in the medium, they were fixed with Viton O-rings (Grainger, MO). The plate was sterilized under a UV lamp for 24 h. Nanofiber meshes without drug were also prepared, and their cellular responses were examined and compared with those of test samples.

2.6.3. Studies on the Endothelial Cell Proliferation Rate. The proliferation rate of endothelial cells upon exposure to various nanoparticles and nanofiber formulations was evaluated using Alamar Blue Assay (Life Technology, CA).[36] Briefly, the proper amount of cells (5,000 cells/well in 200 μL) was seeded onto various formulations loaded in each well of the plate, such as collagen-coated glasses, tissue culture-treated plate (TCP), blank nanofiber and nanofiber with β-estradiol. The plate was incubated for 24 h to allow cells to fully attach to varying substrates.

After the incubation, the medium was removed and 9% Alamar Blue solution (200 μL each) was added to each well. The plate was further incubated for 5 h to allow viable cells to react with the Alamar Blue agent. 5% solution (10 μL) from the plate was taken and transferred to a fresh 96-well plate, to which 90 μL of the fresh medium was added. The proliferation rates were examined every two days using the multireader plate (Ex, 540 nm, and Em, 590 nm). The plate containing test formulations was replenished with the same volume of the fresh medium (10 μL) after each sampling.

2.6.4. Cellular Cytotoxicity against Reactive Oxygen Species (ROS). LDH assay (CytoTox-ONE Homogeneous Membrane Integrity Assay, Promega Co.) was used to determine the lethal concentration (LC50) of exogeneous hydrogen peroxide (external H_2O_2). In brief, cells (10,000 cells/well) seeded on a 96-well plate were incubated for 24 h to allow cells to thoroughly attach to the bottom of the plate. Various concentrations (0 mM to 1.0 mM) of external H_2O_2 were applied to each well, and the plate was incubated for 4 h at 37 °C. After incubation, the plate was equilibrated for 20 min at room temperature.

The equivalent amount of LDH reagent to the medium volume was pipetted into each well and incubated for 10 min. For the measurement of the LDH values, cells were mixed with the lysis buffer, and then the fluorescent intensity (Ex, 560 nm; Em, 590 nm) of each plate was read using the multimode detector (DTX 880, Beckman Coulter Inc., CA).

2.6.5. Effects of β-Estradiol on Cellular Cytotoxicity Induced by ROS. The effects of estrogen on cellular cytotoxicity induced by ROS were evaluated to determine whether or not estrogen is able to prevent cellular redox changes induced by ROS and to elucidate its neuroprotective mechanisms. hPCECs (from ATCC) seeded onto nanofiber meshes spun on circular glasses were treated with exogenous H_2O_2 (0 μM to 1.0 mM in the presence of β-estradiol (0 μM and 0.5 mM). The plate was incubated for 4 h at 37 °C, and the medium was transferred into a fresh 96-well plate. The LDH assay as described in the previous section was used to evaluate the effects of β-estradiol on cellular cytotoxicity induced by ROS.

2.6.6. Assessment of the Amount of Nitric Oxide (NO). Nitric oxide (NO) produced through cellular interaction with β-estradiol was quantified using the Griess assay.[32] The Griess reagent was prepared by mixing of 0.1% *N*-(1-naphthyl)ethylenediamine dihydrochloride (NED) dissolved in DI water and 1% sulfanilamide dissolved in 5% (v/v) phosphoric acid solution.

The medium solution (100 μL) containing 10,000 cells/well was seeded onto electrospun nanofibers placed on a circular coverslip. The plate was incubated overnight to allow cells to attach to fiber matrix. All the medium in the plate was transferred to a fresh 96-well plate, and each well was replenished with the same volume of the fresh cell medium. The plate containing the medium was left at room temperature to allow them to reach an equilibrium state. 1% sulfanilamide solution (50 μL) was added to each well, and the plate was incubated for 5 min at room temperature. Then, 0.1% NED solution (50 μL) was added to each well. The absorbance was measured at 550 nm using the multimode detector and extrapolated to the concentration of NO (μM).

2.7. Statistical Analysis. All data were presented as the means (±SD). Statistical significance was determined using SPSS software (SPSS, Chicago, IL). A P value of less than 0.05 was reported as statistically significant.

3. RESULTS AND DISCUSSION

3.1. Characterization of Nanoparticles. The results of the physical characteristics of ES-NP including an average size, polydispersity index (PDI) and zeta potential, are shown in Table 1B. ES was chosen due to its unique dissolution behavior under varying pH environment.[30] ES-NP were sparsely dissolved in acidic solution and, thus, stable under the acidic condition in which the layer modification with chitosan occurred, whereas they are well dissoluble (whose rate can be properly controllable and sustainable) in neutral pH of blood. Nanoparticles (NP)

produced with the quasi-emulsification technique displayed narrow particle size distribution and homogeneous morphological appearance. NP offered high entrapment efficiency (73.6 ± 1.4%), high loading doses (781.9 ± 39.4 μg) and yield percentage (~70%) of β-estradiol.

The results of zeta-potential measurement demonstrated that negative charges accumulated on the nanoparticle surface (−12.9 ± 1.2 mV) were converted into positive charges (+18.1 ± 0.8 mV) upon the surface of nanoparticles being coated with a chitosan layer. This conversion is mainly due to the interaction between positively charged chitosan in the SA buffer solution and negative charges on the surface of PLGA nanoparticles.

An extra chitosan layer allows core functionality to work on a variety of platforms without losing its main activity. In addition, an increase in the particle size and enhanced loading dose were observed from the nanoparticles modified with a chitosan layer, which helps an excess amount of the drug to be dispersed in the matrix.

3.2. The Degradation Rates of Nanoparticles. Most ES-NP were suitably incorporated through the electrospinning technique within nanofiber meshes. When ES-NP is straightforwardly exposed to the organic solvent (instead of being dispersed in water first) during the nanofiber fabrication process, ES-NP gradually degraded as ES-NP is not stable in the organic solvents including HFIP, which is known as a water-miscible volatile solvent. The degradation rates of ES-NP calculated based on the drug concentration in HFIP solvent are summarized in Table 1 and Figure 2. ES-NP were more stable in the formulation type

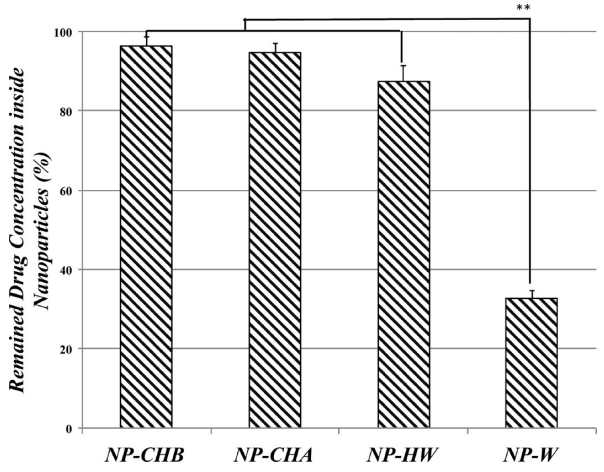

Figure 2. The degradation rate of ES-NP calculated based on the drug concentration in HFIP solvent. Data are shown with mean ± SD ($n = 3$). ** indicates statistically significant difference at $p < 0.01$.

of NP-HW or NP-W (i.e., ES-NP were dispersed in DI water (500 μL), which was mixed with HFIP (1:1 (v/v)) as compared with those directly exposed to HFIP, indicating that as the percentage of HFIP in the solvent decreased (from 100 to 50%), the degradation rate of nanoparticles in the mixture solvent decreased, resulting in a greater amount of intact ES-NP entrapped in nanofibers.

The amount of β-estradiol loaded in the formulation type of NP-HW (i.e., ES-NP were dispersed in H_2O, which was mixed with HFIP (1:1 (v/v)) already containing 15% PLGA) was about 672.25 ± 31.4 μg (87.4 ± 4.1% of the loading dose), whereas that in the formulation type of NP-W was 252.2 ± 15.7 μg, which was 32.6 ± 2.0% of the loading dose. Since ES-NP (i.e., dispersed in H_2O) was added to HFIP solution already containing 15% (w/v) of PLGA, in which PLGA (water-insoluble polymer) was precipitated and lowered the solvent capacity of HFIP solution, the stability of NP-HW significantly increases as compared with NP-W.

In NP-CHA and NP-CHB, ES-NP were fabricated with a chitosan layer that offered extra protection from HFIP, significantly enhancing the drug loading capacity as well as its stability. Based on these results, the potential strategies for stabilizing nanoparticles could include (1) lower organic solvent portion, (2) polymeric transformation and (3) layer modification with more stable polymer to organic solvent.

3.3. Morphological Assessment of Nanoparticles. The morphological status of ES-NP loaded with fluorescent dye (Nile-Red) was examined using fluorescent light microscopy and confocal microscopy. As shown in Figure 3A, the morphological appearance and shapes of ES-NP in both NP-CHA and NP-HW were homogeneous, and numerous red dots reflecting ES-NP were observed. However, in NP-W, only clear nanofiber with red fluorescence (and fewer red dots) from Nile-Red was observed. As previously explained, since ES-NP in NP-W were less stable than those in NP-HW, the amount of nanoparticles entrapped inside nanofibers of NP-W was less than those of NP-HW.

The confocal microscopy study showed similar results to those from fluorescent light microscopy as shown in Figure 3B. In principle, since the confocal microscope can represent both the fluorescence mode and the reflected light mode, there are changes in two image characteristics of a confocal microscope: enhanced lateral and axial resolution. Images of NP-CHA showed markedly improved contrast with the multiphoton excitation microscope than those from NP-HW, indicating that an additional degradation of ES-NP occurred in NP-HW during the electrospinning process as compared with NP-CHA.

3.4. Characterization of Stent Coated with Nanofibers. The stent was suitably coated with nanofibers through the electrospinning technique. The two-step process was applied to coat the inside and the outside of the stent, offering manifest benefits, such as ease in fabrication procedure, and thorough and homogeneous surface coverage. The characteristics of four different types of stent surface coating through the electrospinning technique are compared in Table 1. Bare NF (BNF: nanofiber without ES-NP) had a low yield (49.8 ± 1.2%) and low drug-loading amount (74.6 ± 18.5 μg) as compared with other formulations under the same processing conditions.

Among composite nanofibers with nanoparticles, NP-CHB has offered the maximal yield and drug-loading amount of 66.5 ± 3.7% and 147.9 ± 10.1 μg, respectively. It was also found that NP-CHB on metallic mandrel displayed the most homogeneous coating status (i.e., allotment and homogeneity) compared to the rest of the fabrication types. The results are in good agreement with the previous report on PLGA/PLA blend nanofibers, whose viscosity was greater than that of individual PLGA and PLA.[37] A higher viscosity subsequently improved the positive processing parameters of electrospinnability, offering the maximal yield.

3.5. Structural Variances of Nanofibers. Morphological studies on nanofiber meshes through SEM and TEM image analyses were performed to determine the nanosized structural variations of nanofiber as shown in Figure 4. TEM images (Figure 4C) indicated that the morphology of nanofiber is greatly influenced by the presence of particles inside nanofiber meshes, which were also in good agreement with the SEM results (Figure 4D).

The average fiber diameter (mean ± nm) of three formulations was calculated using the ImageJ program provided from NIH.

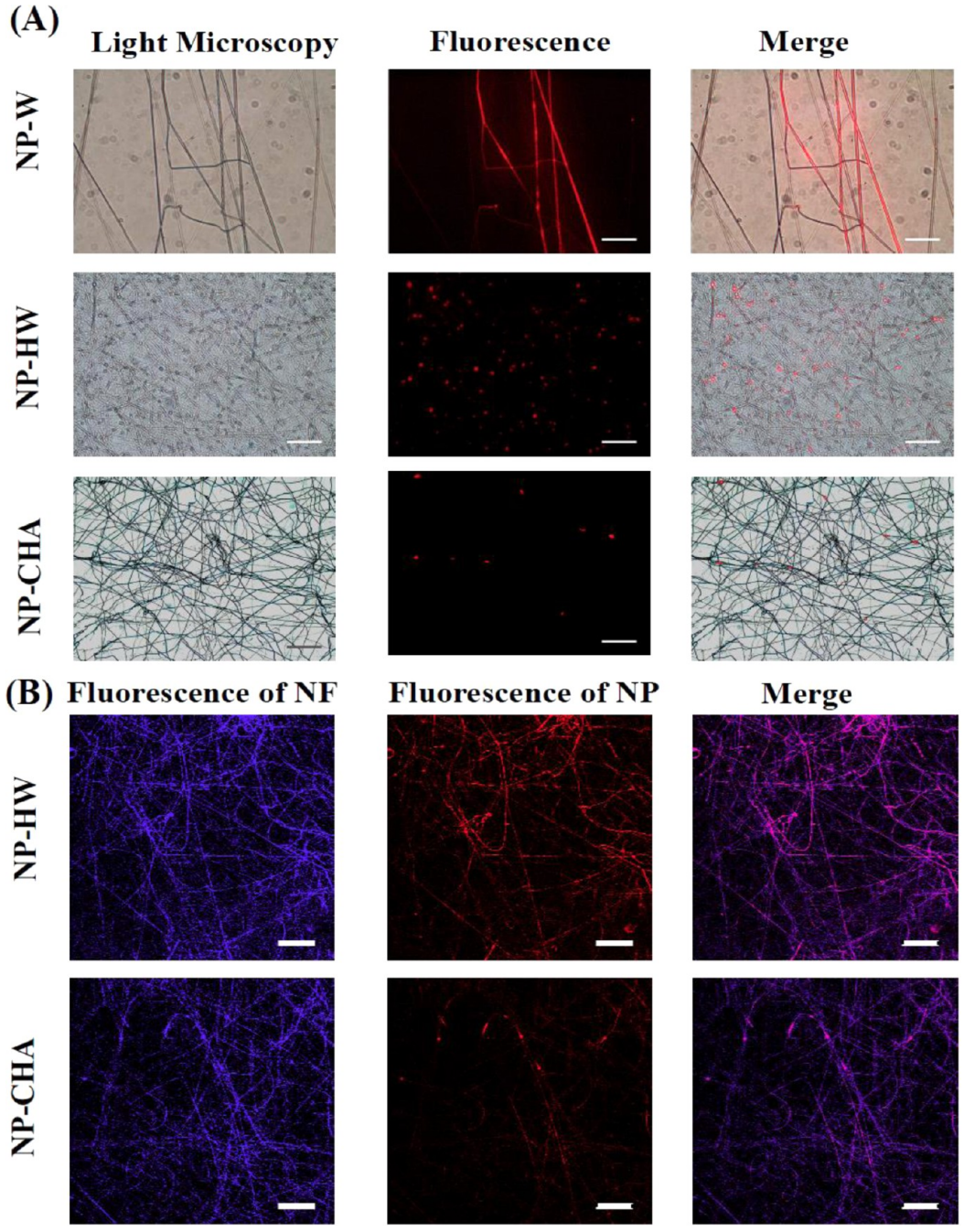

Figure 3. Assessment of the degradation rate of nanoparticles. (A) Fluorescence detection of Nile-Red in ES-NP incorporated in nanofibers. White scale bars indicate the length of 50 μm. (B) Detection of core part of Nile-Red loaded ES-NP sheath (autofluorescence from nanofibers) by confocal microscopy. White scale bars on right bottom indicate the length of 30 μm.

As shown in Figure 4D, the average diameter of all types of nanofibers ranged from 250 to 530 nm. A large diameter of nanofiber was observed from NP-CHA, some of whose widths are greater than 1 μm.

The distribution profiles of the diameter (δ) varied among BNF, NP-HW and NP-CHA. BNF had the smallest standard deviation value of δ (less than 100 nm), whereas NP-HW and NP-CHA had a large distribution value on the histogram (δ is greater than 127.9 nm). These findings indicated that the major source of wide diameter distribution of NP-HW and NP-CHA might stem from a broad polydispersity index (PDI) of the nanoparticles, as the diameter of the nanoparticles was greatly influenced by the entrapment space in the fiber mesh.

3.6. Degradation Profiles of Nanofiber-Coated Formulations. The polymeric degradation rate was examined based on weight loss at specific time intervals. As shown in Figure 5, about 10% of the initial weight was lost from three formulations for 14 days. After that point, the weight loss of NP-CHA was accelerated and reached up to 60% of loss within 4 weeks, whereas NP-HW showed only 50% weight loss in 4 weeks. The accelerated degradation seems to be mainly due to the presence of chitosan derivatives in NP-CHA, whose high swelling property could absorb the significant amount of water. The swelling property of chitosan seems to trigger fast hydrolysis of PLGA.

In contrast, the weight loss of NP-CHB blended with PLGA and PLA was about 40% of the initial weight, which was 20%

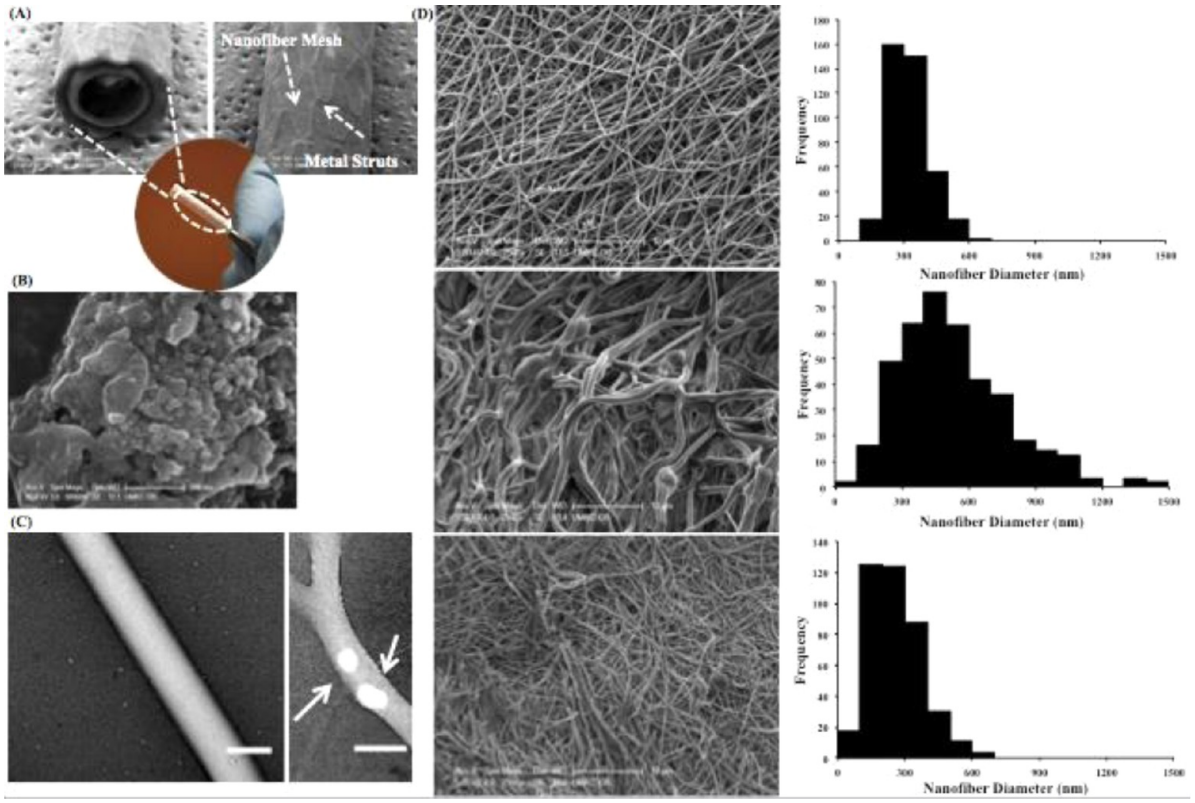

Figure 4. Morphological studies on stent coated with nanofiber: (A) SEM results of stent surface coated with nanofiber. Top, the front view of the stent. Bottom, the side view of the stent. (B) SEM images of ES-NP. (C) TEM images of ES-NP. Left, bare nanofiber (BNF). Right, nanofiber containing nanoparticles (NP-HW). Arrows point to nanoparticles inside nanofibers. White scale bars indicate the length of 20 nm. (D) SEM images of three nanofiber formulations. Top, bare nanofiber (BNF). Middle, nanofiber with nanoparticles (NP-HW). Bottom, nanofiber with nanoparticles layered by chitosan (NP-CHA).

lower than that of NP-CHA. As previously reported, PLA blending increased the hydrophobicity on the surface of nanofiber, reducing the hydrolysis rate of PLGA in NP-CHB.[37]

3.7. The Mechanical Properties of Nanofiber Formulations. The stress−strain curves of various nanofiber formulations are shown in Figure 5B. NP-HW and NP-CHA displayed low yield points and elongation rates. The stress curve sharply decreased right after the yield point. For NP-CHB, it had a relatively high yield point and an elongation rate. The stress gradually reduced and reached an equilibrium status. As the strain rate further increased, the stress rather decreased. Thus, it is expected that stent coated with NP-CHB could yield a relatively high elongation rate and stability at body temperature.

3.8. In Vitro Release Profile of β-Estradiol. The release profiles of β-estradiol from stents coated with varying types of nanofibers were investigated under the simulated physiological conditions (as shown in Figure 6). To prevent the drug loss from the light, all the experiments were conducted in the dark room with the incubator continuously rotating at 120 rpm. For bare NF (BNF), about 50% of β-estradiol was released from the stent within a week and all loaded β-estradiol was released from the stent in 4 weeks (Figure 6). However, it took a longer period (about 2 weeks) for NP-HW to release 50% of β-estradiol from the stents as compared with BNF.

NP-CHA offered a sustained release profile of β-estradiol. During the first seven days, the drug release profile of β-estradiol gradually increased (without any burst release), and then reached the equilibrium state. There was no significant difference in the release profiles between NP-CHA and NP-CHB. The chitosan layer modification of nanoparticles offered more sustained release profiles of β-estradiol than other formulations. Therefore, an incorporation of the nanoparticles inside nanofibers seems to be an ideal strategy for stent coating, achieving a sustained release profile of β-estradiol.

3.9. Effects of β-Estradiol on the Proliferation Rates of hPCECs. The proliferation rates of hPCECs seeded on various biocompatible substrates were monitored using the Alamar Blue assay. The fluorescent readings based on the fluorescent unit assessed on the first day were normalized for the measurement of the proliferation rate.

As shown in Figure 7, β-estradiol increased the proliferation rate of hPCECs. It was found that the proliferation rate of hPCECs on the glass coverslip coated with collagen was similar to those on tissue culture-treated plate (TCP). However, the proliferation rate of hPCECs induced by BNF (i.e., nanofibers without β-estradiol) was significantly lower than those induced by other groups (glass coated by collagen, TCP and nanofibers with β-estradiol). It was also observed that nanofibers incorporated with ES-NP containing β-estradiol yielded a high endothelial proliferation rate, which was about 3-fold greater than that of the control formulation (i.e., BNF). It can be concluded that nanofibers incorporated with ES-NP containing β-estradiol could achieve enhanced endothelialization at the blood vessels and greatly relieve any side effects induced by implanted drug eluting stent.

3.10. Effects of β-Estradiol on Externally-Induced ROS. To evaluate the effects of β-estradiol (0 and 0.5 mM) on the ROS regulation, nanofiber meshes spun onto circular cover glasses

dx.doi.org/10.1021/mp400231p | Mol. Pharmaceutics 2013, 10, 4432−4442

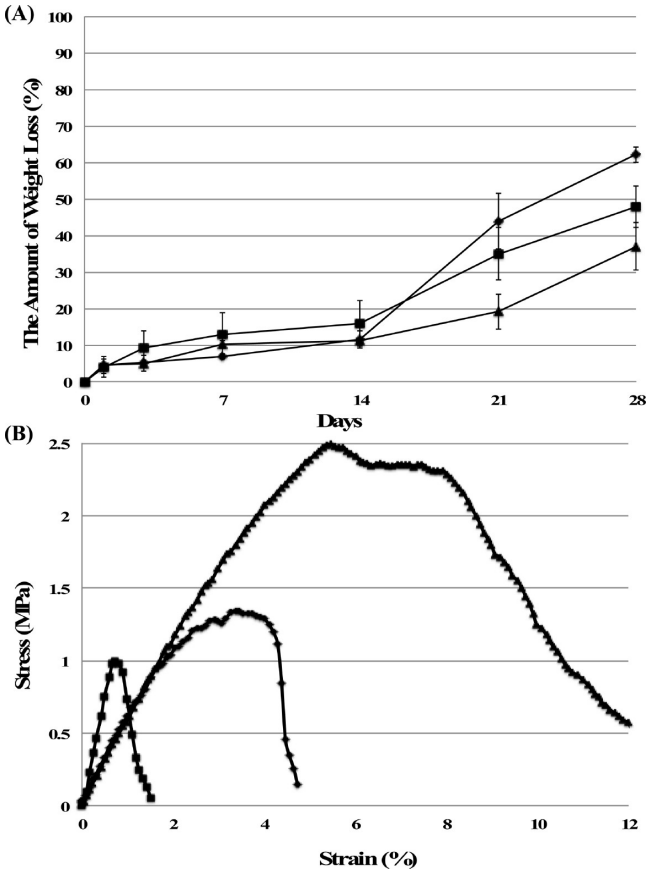

Figure 5. The degradation rates of nanofibers (A) (n = 3) and mechanical property curve (B): ■, NP-HW; ◆, NP-CHA; ▲, NP-CHB.

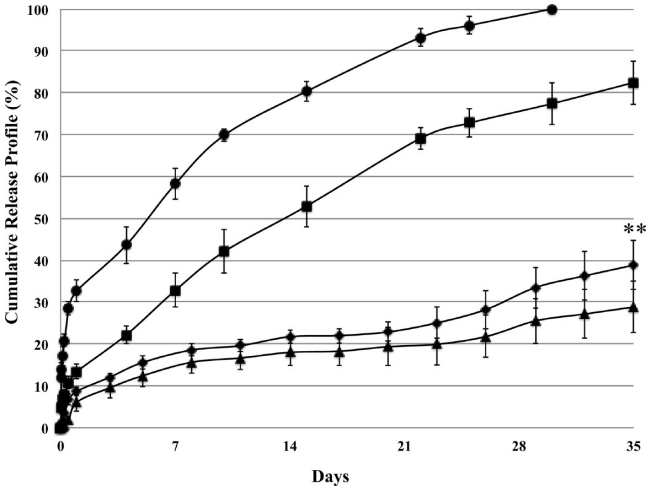

Figure 6. The cumulative amount of β-estradiol release profiles. There are significant differences in the cumulative amounts of β-estradiol among formulation types (NP-CHA and NP-CHB vs BNF and NP-HW, ** indicates statistically significant difference at $p < 0.01$, $n = 3$). ●: BNF. ■: NP-HW. ◆: NP-CHA. ▲: NP-CHB.

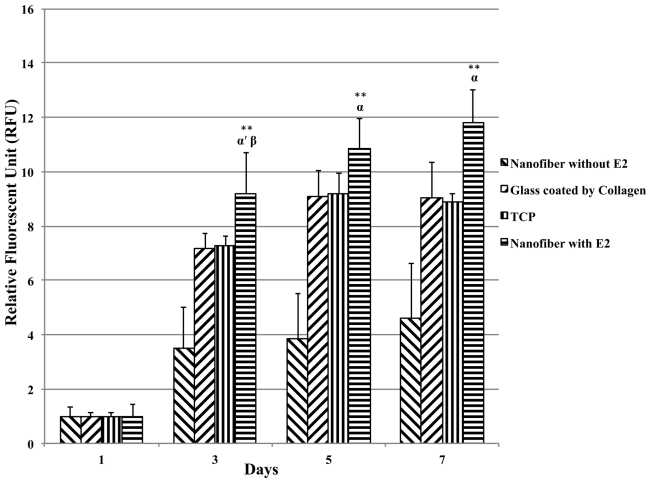

Figure 7. Effects of β-estradiol on the proliferation rates of hPCECs (n = 6). ** indicates that there are significant differences in the rates between NP-CHB with and without β-estradiol ($p < 0.01$). α indicates that there is a significant difference between NP-CHB with β-estradiol and tissue culture-treated plate (TCP) (α, $p < 0.05$; α', $p < 0.01$). β indicates statistically significant difference between NP-CHB with β-estradiol and glass coated by collagen.

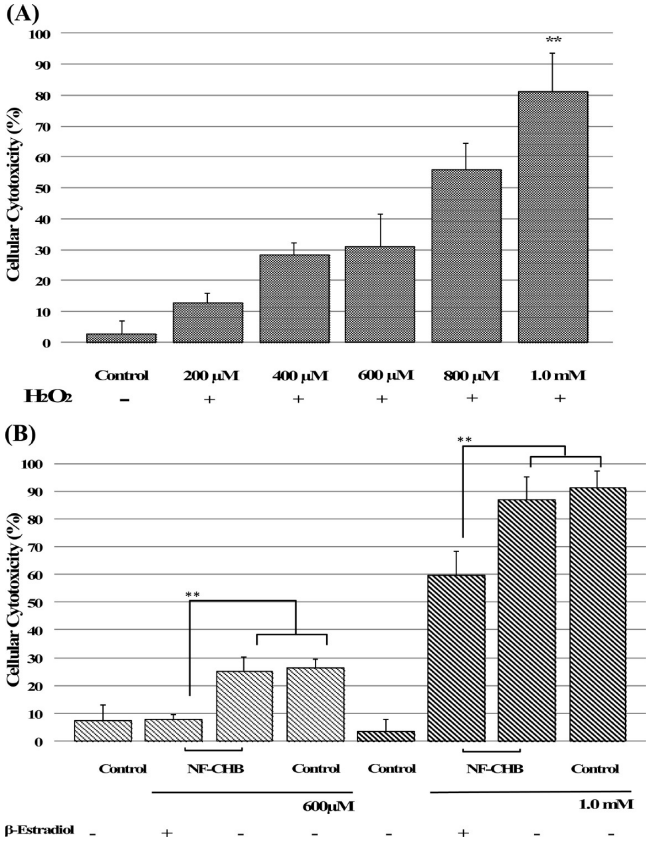

Figure 8. Effects of β-estradiol on cellular cytotoxicity of endothelial cells against externally induced reactive oxygen species (ROS). (A) Cellular apoptosis rates induced by H_2O_2 varied ranging from 200 μM to 1.0 mM (** statistically significant difference, $p < 0.01$, n = 8). (B) Cellular cytotoxic profiles with two different concentrations of H_2O_2 (600 μM and 1.0 mM) (**statistically significant difference at $p < 0.05$, n = 5).

were initially treated with varying doses of H_2O_2 (0 μM to 1.0 mM). Cellular cytotoxicity against externally induced ROS was evaluated using the LDH assay. As shown in Figure 8A, the cytotoxic response increased, as the level of H_2O_2 applied to the system increased. The LC50 of H_2O_2 was about 800 μM (31.2 ± 10.4% for 600 μM and 56.1 ± 8.2% for 800 μM). The cytotoxic response sharply increased with higher concentrations of H_2O_2 than 800 μM, and the cells treated with H_2O_2 at concentrations greater than 1 mM were mostly nonviable (81.1 ± 12.4%,

dx.doi.org/10.1021/mp400231p | Mol. Pharmaceutics 2013, 10, 4432−4442

$p < 0.01$), indicating that ROS induces cell apoptosis and causes the rupture of atheroma thin layer in a concentration dependent manner.

As shown in Figure 8B, β-estradiol (0.5 mM) reduced cellular cytotoxicity from 25.2 ± 4.9% to 8.1 ± 1.4% in the presence of H_2O_2 (600 μM) and from 86.8 ± 8.4% to 59.4 ± 8.7% in the presence of 1.0 mM H_2O_2, suggesting that β-estradiol efficiently alleviated ROS induced cytotoxicity in hPCECs. The formulation itself had no cytotoxic effect on cells, as its viability is almost same as that of the positive control. Therefore, nanofiber-based formulations having the sustained release profiles of β-estradiol could serve as a suitable platform for protection of hPCECs from ROS induced cytotoxicity.

3.11. Effects of β-Estradiol on Production of Nitric Oxide (NO). Giress reagent assay was used to assess the amount of nitric oxide (NO) produced by hPCECs. As shown in Figure 9,

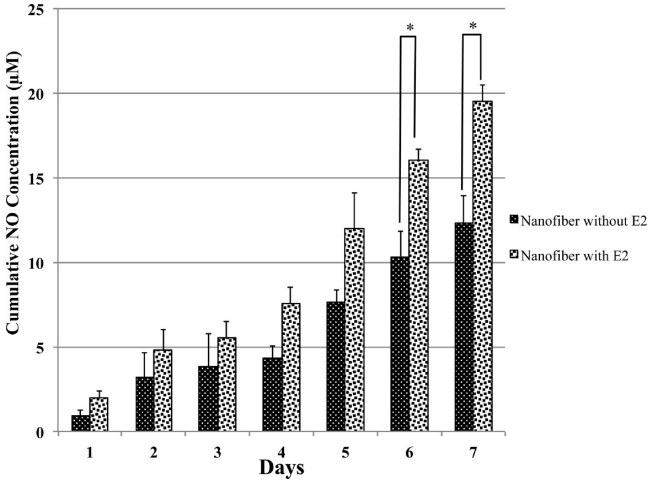

Figure 9. Effects of β-estradiol on production of nitric oxide (NO). Data expressed as mean ± SD; $n = 5$, * indicates statistically significant difference at $p < 0.05$.

the amounts of NO production by hPCECs in the presence of β-estradiol, 16.1 ± 0.6 μM (6 days) and 19.5 ± 0.9 μM (7 days), were much greater than those of the control (i.e., without β-estradiol) (10.3 ± 1.4 μM and 12.3 ± 1.6 μM for 6 days and 7 days, respectively, $p < 0.05$). These results are well correlated with the previous studies, in which the proliferation rate of hPCECs seeded on the nanofibers with β-estradiol was significantly greater than that of the control.

An integral attribute of β-estradiol to the treatment of in-stent restenosis is to protect the endothelial cells from the stress induced by ROS and stimulate NO production. In addition, the clinical study with β-estradiol confirmed that there are no obvious side effects, such as cancer, venous thromboembolism or stroke.[19] Since NO is a powerful endogenous vasodilator and has various physiological functions, the enhanced amount of NO by external stimuli, such as β-estradiol, efficiently preserves the cell proliferation rate and subsequently regulates the blood flow and the endothelialization process. Toward these efforts, the delivery strategy based on the mixture of NO donors and β-estradiol is currently being explored to prevent in-stent restenosis, guaranteeing great benefit to atherosclerosis treatment.

4. CONCLUSION

Nanofiber was explored as a stent surface coating substance for the treatment of coronary artery diseases (CAD). Stent was surface-coated with nanofibers produced by electrospinning technique through the two-step process. Among composite nanofibers loaded with nanoparticles, NP-CHB has offered the maximal yield and drug-loading amount due to maintenance of high coating stability. Nanofibers incorporated with β-estradiol offered a high endothelial proliferation rate and efficiently regulated the reactive oxygen species (ROS) at the subcellular level. The results of this study guarantee further application of nanofibers loaded with β-estradiol-containing nanoparticles for the surface coating of cardiovascular stent, potentially achieving enhanced endothelialization at the implanted sites of blood vessels.

AUTHOR INFORMATION

Corresponding Author

*2464 Charlotte Street, HSB-4242, Division of Pharmaceutical Sciences, University of Missouri at Kansas City, Kansas City, MO 64108. Tel: 816-235 2408. Fax: 816-235-5779. E-mail: leech@umkc.edu.

Notes

The authors declare no competing financial interest.

REFERENCES

(1) Halon, D. A.; Adawi, S.; Dobrecky-Mery, I.; Lewis, B. S. Importance of increasing age on the presentation and outcome of acute coronary syndromes in elderly patients. *J. Am. Coll. Cardiol.* **2004**, *43* (3), 346−52.

(2) Tanous, D.; Brasen, J. H.; Choy, K.; Wu, B. J.; Kathir, K.; Lau, A.; Celermajer, D. S.; Stocker, R. Probucol inhibits in-stent thrombosis and neointimal hyperplasia by promoting re-endothelialization. *Atherosclerosis* **2006**, *189* (2), 342−9.

(3) Roger, V. L.; Go, A. S.; Lloyd-Jones, D. M.; Benjamin, E. J.; Berry, J. D.; Borden, W. B.; Bravata, D. M.; Dai, S.; Ford, E. S.; Fox, C. S.; Fullerton, H. J.; Gillespie, C.; Hailpern, S. M.; Heit, J. A.; Howard, V. J.; Kissela, B. M.; Kittner, S. J.; Lackland, D. T.; Lichtman, J. H.; Lisabeth, L. D.; Makuc, D. M.; Marcus, G. M.; Marelli, A.; Matchar, D. B.; Moy, C. S.; Mozaffarian, D.; Mussolino, M. E.; Nichol, G.; Paynter, N. P.; Soliman, E. Z.; Sorlie, P. D.; Sotoodehnia, N.; Turan, T. N.; Virani, S. S.; Wong, N. D.; Woo, D.; Turner, M. B.; American Heart Association Statistics, C.; Stroke Statistics, S. Heart disease and stroke statistics−2012 update: a report from the American Heart Association. *Circulation* **2012**, *125* (1), e2−e220.

(4) Lusis, A. J. Atherosclerosis. *Nature* **2000**, *407* (6801), 233−41.

(5) Stary, H. C. Natural history and histological classification of atherosclerotic lesions: an update. *Arterioscler. Thromb. Vasc. Biol.* **2000**, *20* (5), 1177−8.

(6) Patel, M. R.; Dehmer, G. J.; Hirshfeld, J. W.; Smith, P. K.; Spertus, J. A. ACCF/SCAI/STS/AATS/AHA/ASNC 2009 Appropriateness Criteria for Coronary Revascularization: a report by the American College of Cardiology Foundation Appropriateness Criteria Task Force, Society for Cardiovascular Angiography and Interventions, Society of Thoracic Surgeons, American Association for Thoracic Surgery, American Heart Association, and the American Society of Nuclear Cardiology Endorsed by the American Society of Echocardiography, the Heart Failure Society of America, and the Society of Cardiovascular Computed Tomography. *J. Am. Coll. Cardiol.* **2009**, *53* (6), 530−53.

(7) Byrne, R. A.; Joner, M.; Tada, T.; Kastrati, A. Restenosis in bare metal and drug-eluting stents: distinct mechanistic insights. *Minerva Cardioangiol.* **2012**, *60* (5), 473−89.

(8) Bonaventura, K.; Leber, A. W.; Sohns, C.; Roser, M.; Boldt, L. H.; Kleber, F. X.; Haverkamp, W.; Dorenkamp, M. Cost-effectiveness of paclitaxel-coated balloon angioplasty and paclitaxel-eluting stent implantation for treatment of coronary in-stent restenosis in patients with stable coronary artery disease. *Clin. Res. Cardiol.* **2012**, *101* (7), 573−84.

(9) Vedantham, K.; Chaterji, S.; Kim, S. W.; Park, K. Development of a probucol-releasing antithrombogenic drug eluting stent. *J. Biomed. Mater. Res., Part B* **2012**, *100* (4), 1068−77.
(10) Thierry, B.; Winnik, F. M.; Merhi, Y.; Silver, J.; Tabrizian, M. Bioactive coatings of endovascular stents based on polyelectrolyte multilayers. *Biomacromolecules* **2003**, *4* (6), 1564−71.
(11) Liistro, F.; Angioli, P.; Bellandi, G.; Bolognese, L.; Ducci, K.; Porto, I.; Turini, F.; Ventoruzzo, G. TCT-343 Paclitaxel Drug Eluting Balloon Versus Standard Angioplasty To Reduce Restenosis In Diabetic Patients With In Stent Restenosis Of The Superficial Femoral And Proximal Popliteal Artery. *J. Am. Coll. Cardiol.* **2012**, *60*, 17.
(12) Yuk, S. H.; Oh, K. S.; Park, J.; Kim, S. J.; Kim, J.; Kwon, J. H. I. K. Paclitaxel-loaded poly(lactide-co-glycolide)/poly(ethylene vinyl acetate) composite for stent coating by ultrasonic atomizing spray. *Sci. Technol. Adv. Mater.* **2012**, *13* (2), 025005.
(13) Schierbeck, L. L.; Rejnmark, L.; Tofteng, C. L.; L., S.; Eiken, P.; L Mosekilde, L.; Køber, L.; Beck Jensen, J. E. Effect of hormone replacement therapy on cardiovascular events in recently postmenopausal women: randomised trial. *BMJ* **2012**, *345*, e6409.
(14) Airoldi, F.; Di Mario, C.; Ribichini, F.; Presbitero, P.; Sganzerla, P.; Ferrero, V.; Vassanelli, C.; Briguori, C.; Carlino, M.; Montorfano, M.; Biondi-Zoccai, G. G.; Chieffo, A.; Ferrari, A.; Colombo, A. 17-beta-estradiol eluting stent versus phosphorylcholine-coated stent for the. *Am. J. Cardiol.* **2005**, *96* (5), 664−7.
(15) Wang, J.; Green, P. S.; Simpkins, J. W. Estradiol protects against ATP depletion, mitochondrial membrane potential. *J. Neurochem.* **2001**, *77* (3), 804−11.
(16) Wing, L. Y.; Chen, Y. C.; Shih, Y. Y.; Cheng, J. C.; Lin, Y. J.; Jiang, M. J. Effects of oral estrogen on aortic ROS-generating and -scavenging enzymes and atherosclerosis in apoE-deficient mice. *Exp. Biol. Med. (Maywood)* **2009**, *234* (9), 1037−46.
(17) Irani, K. Oxidant signaling in vascular cell growth, death, and survival: a review of the. *Circ. Res.* **2000**, *87* (3), 179−83.
(18) Bombeli, T.; Karsan, A.; Tait, J. F.; Harlan, J. M. Apoptotic vascular endothelial cells become procoagulant. *Blood* **1997**, *89* (7), 2429−42.
(19) Schierbeck, L. L.; Rejnmark, L.; Tofteng, C. L.; Stilgren, L.; Eiken, P.; Mosekilde, L.; Kober, L.; Jensen, J. E. Effect of hormone replacement therapy on cardiovascular events in recently postmenopausal women: randomised trial. *BMJ* **2012**, *345*, e6409.
(20) Yi, L.; Chen, C. Y.; Jin, X.; Zhang, T.; Zhou, Y.; Zhang, Q. Y.; Zhu, J. D.; Mi, M. T. Differential suppression of intracellular reactive oxygen species-mediated signaling pathway in vascular endothelial cells by several subclasses of flavonoids. *Biochimie* **2012**, *94* (9), 2035−44.
(21) Taskiran, D.; Evren, V. Estradiol protects adipose tissue-derived stem cells against H(2)O(2)-induced toxicity. *J. Biochem. Mol. Toxicol.* **2012**, *26* (8), 301−7.
(22) Kim, J. K.; Pedram, A.; Razandi, M.; Levin, E. R. Estrogen prevents cardiomyocyte apoptosis through inhibition of reactive oxygen species and differential regulation of p38 kinase isoforms. *J. Biol. Chem.* **2006**, *281*, 6760−7.
(23) Song, J. Y.; Kim, M. J.; Jo, H. H.; Hwang, S. J.; Chae, B.; Chung, J. E.; Kwon, D. J.; Lew, Y. O.; Lim, Y. T.; Kim, J. H.; Kim, M. R. Antioxidant effect of estrogen on bovine aortic endothelial cells. *J. Steroid Biochem. Mol. Biol.* **2009**, *117*, 74−80.
(24) Chen, H. Y.; Zhang, X.; Chen, S. F.; Zhang, Y. X.; Liu, Y. H.; Ma, L. L.; Wang, L. X. The protective effect of 17beta-estradiol against hydrogen peroxide-induced apoptosis on mesenchymal stem cell. *Biomed. Pharmacother.* **2012**, *66* (1), 57−63.
(25) Abizaid, A.; Albertal, M.; Costa, M. A.; Abizaid, A. S.; Staico, R.; Feres, F.; Mattos, L. A.; Sousa, A. G.; Moses, J.; Kipshidize, N.; Roubin, G. S.; Mehran, R.; New, G.; Leon, M. B.; Sousa, J. E. First human experience with the 17-beta-estradiol-eluting stent: the Estrogen And Stents To Eliminate Restenosis (EASTER) trial. *J. Am. Coll. Cardiol.* **2004**, *43*, 1118−21.
(26) Abizaid, A.; Chaves, A. J.; Leon, M. B.; Hauptmann, K.; Mehran, R.; Lansky, A. J.; Baumbach, W.; Shankar, H.; Muller, R.; Feres, F.; Sousa, A. G.; Sousa, J. E.; Grube, E. Randomized, double-blind, multicenter study of the polymer-based 17-beta estradiol-eluting stent for treatment of native coronary artery lesions: six-month results of the ETHOS I trial. *Catheterization Cardiovasc. Interventions* **2007**, *70* (5), 654−60.
(27) Ryu, S. K.; Mahmud, E.; Tsimikas, S. Estrogen-eluting stents. *J Cardiovasc. Transl. Res.* **2009**, *2* (3), 240−4.
(28) Farhatnia, Y.; Tan, A.; Motiwala, A.; Cousins, B. G.; Seifalian, A. M. Evolution of covered stents in the contemporary era: clinical application, materials and manufacturing strategies using nanotechnology. *Biotechnol. Adv.* **2013**, *31* (5), 524−42.
(29) Grabovac, V.; Bernkop-Schnurch, A. Development and in vitro evaluation of surface modified poly(lactide-co-glycolide) nanoparticles with chitosan-4-thiobutylamidine. *Drug Dev. Ind. Pharm.* **2007**, *33* (7), 767−74.
(30) Yoo, J. W.; Giri, N.; Lee, C. H. pH-sensitive Eudragit nanoparticles for mucosal drug delivery. *Int. J. Pharm.* **2011**, *403* (1−2), 262−7.
(31) Qian, J.; Zhang, Q.; Church, J. E.; Stepp, D. W.; Rudic, R. D.; Fulton, D. J. Role of local production of endothelium-derived nitric oxide on cGMP signaling and S-nitrosylation. *Am. J. Physiol.* **2010**, *298* (1), H112−8.
(32) Yoo, J. W.; Lee, J. S.; Lee, C. H. Characterization of nitric oxide-releasing microparticles for the mucosal delivery. *J. Biomed. Mater. Res., Part A* **2010**, *92* (4), 1233−43.
(33) Acharya, G.; Lee, C. H.; Lee, Y. Optimization of cardiovascular stent against restenosis: factorial design-based statistical analysis of polymer coating conditions. *PLoS One* **2012**, *7*, e43100.
(34) Soffer, L.; Wang, X.; Zhang, X.; Kluge, J.; Dorfmann, L.; Kaplan, D. L.; Leisk, G. Silk-based electrospun tubular scaffolds for tissue-engineered vascular grafts. *J. Biomater. Sci., Polym. Ed.* **2008**, *19* (5), 653−64.
(35) Xu, C.; Wang, Y. Cross-linked demineralized dentin maintains its mechanical stability when challenged by bacterial collagenase. *J. Biomed. Mater. Res., Part B* **2011**, *96* (2), 242−8.
(36) Li, M.; Guo, Y.; Wei, Y.; MacDiarmid, A. G.; Lelkes, P. I. Electrospinning polyaniline-contained gelatin nanofibers for tissue engineering applications. *Biomaterials* **2006**, *27* (13), 2705−15.
(37) Liu, H.; Wang, S.; Qi, N. Controllable structure, properties, and degradation of the electrospun PLGA/PLA-blended nanofibrous scaffolds. *J. Appl. Polym. Sci.* **2012**, *125* (S2), 468−476.